



# CHORUS

This is the accepted manuscript made available via CHORUS. The article has been published as:

## Superconductivity in Bi/Ni bilayer system: Clear role of superconducting phases found at Bi/Ni interface

L. Y. Liu, Y. T. Xing, I. L. C. Merino, H. Micklitz, D. F. Franceschini, E. Baggio-Saitovitch, D. C. Bell, and I. G. Solórzano

Phys. Rev. Materials **2**, 014601 — Published 5 January 2018

DOI: [10.1103/PhysRevMaterials.2.014601](https://doi.org/10.1103/PhysRevMaterials.2.014601)

# Superconductivity in Bi/Ni bi-layer system: clear role of superconducting phases found at Bi/Ni interface

L.Y. Liu<sup>1</sup>, Y. T. Xing<sup>2</sup>, I. L. C. Merino<sup>3</sup>, H. Micklitz<sup>3</sup>, D. F. Franceschini<sup>2</sup>, E. Baggio-Saitovitch<sup>3</sup>, D.C. Bell<sup>4,5</sup>, I. G. Solórzano<sup>1</sup>

<sup>1</sup> *Departamento de Engenharia Química e de Materiais,  
Pontifícia Universidade Católica do Rio de Janeiro, Rio de Janeiro, Brasil*

<sup>2</sup> *Instituto de Física da Universidade Federal Fluminense,  
Niterói, 24210-346, Rio de Janeiro, Brasil*

<sup>3</sup> *Centro Brasileiro de Pesquisas Físicas, Rio de Janeiro 22290-180, Brazil*

<sup>4</sup> *Harvard John A. Paulson School of Engineering  
and Applied Sciences, Cambridge MA, USA and*

<sup>5</sup> *Center for Nanoscale Systems, Harvard University, Cambridge MA, USA*

## Abstract

Bi/Ni bi-layers with varying Bi and Ni layer thicknesses have been prepared by (a) pulsed-laser deposition (PLD) at 300 K and (b) thermal evaporation at 4.2 K. A two-step superconducting transition appears on the electrical transport measurements in the samples prepared by PLD. High-resolution transmission and scanning transmission electron microscopy, supported by Energy-Dispersive X-ray Spectroscopy (EDXS) analysis, reveal that two superconducting intermetallic alloys, namely NiBi and NiBi<sub>3</sub>, are formed by interdiffusion, if the bi-layers are prepared at 300 K. The  $T_c$  of the two phases behaves very differently in external magnetic field and the upper critical magnetic fields at zero temperature [ $B_{c2}(0)$ ] were estimated as 1.1 T and 7.4 T, respectively. The lower value corresponds to the  $B_{c2}(0)$  of NiBi<sub>3</sub> phase and higher one is supposed to be of NiBi. These alloys are responsible for the superconductivity and the two-step transition appearing in the Bi/Ni bi-layer system. Surprisingly, the Bi-rich phase (NiBi<sub>3</sub>) is formed near the Ni layer while the Ni-rich phase (NiBi) is formed far from the Ni layer. The EDXS analysis at nanometer scale clearly shows an unusual increase of Ni concentration near the interface of Bi/substrate. The limited thickness of Bi layer in the interdiffusion process results in the unexpected distribution of Ni concentration. Samples prepared at 4.2 K after annealing at 300 K do not show any superconductivity, which indicates that a non-epitaxial Bi/Ni interface does not induce superconductivity in the case interdiffusion does not occur. These results offer a deeper understanding of the superconductivity in the Bi/Ni bi-layer system.

## I. INTRODUCTION

In spite of the fact that crystalline bismuth (Bi) and nickel (Ni) are not superconducting down to 50 mK [1], if one deposits a Ni layer on top of a rhombohedral Bi layer, the bi-layer system becomes a superconductor [2–7]. Since the discovery of superconductivity in this system, there were many different interpretations, but no agreement has been reached up to date [8–10]. It has been shown by Moodera et al. [3] that a novel FCC phase of Bi can be induced by growing Bi on a thin FCC Ni seed layer. This novel phase of Bi exhibits superconductivity with  $T_c \sim 4.2$  K and displays none of the usual features of Bi typically observed in tunneling experiments [2]. In that work, no ferromagnetism was observed with Nickel thicknesses up to  $d_{Ni} \approx 2.0$  nm. P. LeClair reported [4] that with larger Ni thicknesses, there is a narrow range of  $d_{Ni} \approx 2.0 \sim 4.2$  nm where superconductivity is present in the ferromagnetic Ni and that ferromagnetism appears in Ni just above  $d_{Ni} \sim 1.6$  nm. Siva [5] and Chao [11] reported the spontaneous formation of a superconducting  $NiBi_3$  phase in thermally evaporated Bi/Ni bi-layer films. Cross sectional Transmission Electron Microscopy (TEM) and Energy-Dispersive X-ray Spectroscopy (EDXS) results confirmed the mixture of Ni and Bi throughout the top Bi layer. In order to avoid diffusion of Bi atoms in Ni layer and rule out the interpretation with formation of  $NiBi_3$ , Gong et al. prepared Bi/Ni bi-layers at 110 K [6] and they claim that there is no evidence of formation of Bi-Ni intermetallic compounds and that the sample shows superconductivity [6]. There are some other explanations, for example, superconductivity induced by magnetic fluctuation at the interface of Bi/Ni [8], and the formation of a very thin amorphous Bi layer at the interface of Bi and Ni [7], etc. It is for these reasons that there is need for more clear experiments in order to solve the problem for the appearance of superconductivity in this system. Furthermore, both of the intermetallic compounds of Ni and Bi, namely,  $NiBi$  and  $NiBi_3$ , are superconducting [12–19], systematic and detailed studies of the microstructure of Bi/Ni interface are needed to clarify the interpretation of superconductivity in this system. Although some results are based on the Bi/Ni bi-layers prepared at 110 K [6], the possibility of diffusion of Bi atoms cannot be ruled out due to the low melting temperature of Bi. For that reason, sample preparation at even much lower temperature (4.2 K) is necessary in order to have a clean interface of Ni and Bi.

In this work, we have studied the superconducting properties of Bi/Ni bi-layers prepared

at room temperature and at 4.2 K. In all systems the Bi/Ni interface has been investigated systematically by means of High-Resolution Transmission Electron Microscopy (HRTEM).

## II. EXPERIMENTAL

Bi/Ni bi-layers with different thicknesses have been prepared at room temperature by means of pulsed-laser deposition (PLD) using a Nd-YAG laser with 1064 nm wavelength [20]. Since the superconductivity of Bi/Ni bi-layers does not depend on the deposition sequence [6], we deposited the Bi layers first and then the Ni layer on top for all samples in order to prevent the oxidation of the Bi layer. The thickness of the Bi and Ni layers was controlled by the number of laser pulses. After the deposition, electric transport and magnetic properties of the bi-layer systems have been investigated by using Quantum Design Dynacool PPMS. The four-probe method was used in the electric transport measurements with the current direction parallel to the surface of the sample. Cross-section samples for HRTEM and Scanning Transmission Electron Microscopy (STEM) were prepared by a Focused Ion Beam (FIB) system. Since the interesting structure is the interface of Ni and Bi, an amorphous carbon layer was deposited on top of the sample before the FIB fabrication in order to prevent the possible damage induced by the ion beam. Two additional samples have been prepared at 4.2 K using a thermal evaporation system for both Bi and Ni, which is attached to a  $^4\text{He}$  cryostat and contains a cooled substrate at 4.2 K [21, 22]. Pre-deposited contacts on the sapphire substrate allow for in-situ measurement of the electrical resistivity between 2.0 K and 300 K. Samples for HRTEM study have been prepared by FIB, like all the TEM samples in this study.

## III. RESULTS AND DISCUSSION

### A. Samples prepared at room temperature

Fig. 1 shows the resistivity measurements of the Bi/Ni bi-layers prepared at room temperature with different thicknesses. The Bi/Ni samples show superconductivity and the pure Bi does not, as expected. The highest  $T_c$  obtained is that for the sample with 38 nm Bi and 2 nm Ni. Changing Bi or Ni thickness from these values always decreases  $T_c$ . A two-step transition has been observed in Bi38Ni8 and Bi38Ni20 [see Fig. 1(a)]. However, if

the thickness of Ni layer is fixed (2 nm) and varying the thickness of Bi layer, no two-step transition has been observed [see Fig. 1 (b)]. These results show that the two-step transition only occurs for bi-layer systems with thicker Ni layers ( $d_{Ni} \sim 8$  nm). However, if the Ni layer becomes too thick (40 nm), the second transition disappears and the sample does not have a full superconducting transition. Since two superconducting alloys (NiBi and NiBi<sub>3</sub>) exist in Bi/Ni system, the two-step transition observed in this work might be an indication of the NiBi and NiBi<sub>3</sub> formation. Such a co-existence of two superconducting phases in Bi/Ni bi-layers has up to our knowledge not been reported in literature. Therefore this assumption needs more evidence. The sample with a thin Bi layer (6.3 nm) does not show a superconducting transition down to 1.8 K, which also is in agreement with literature [6].

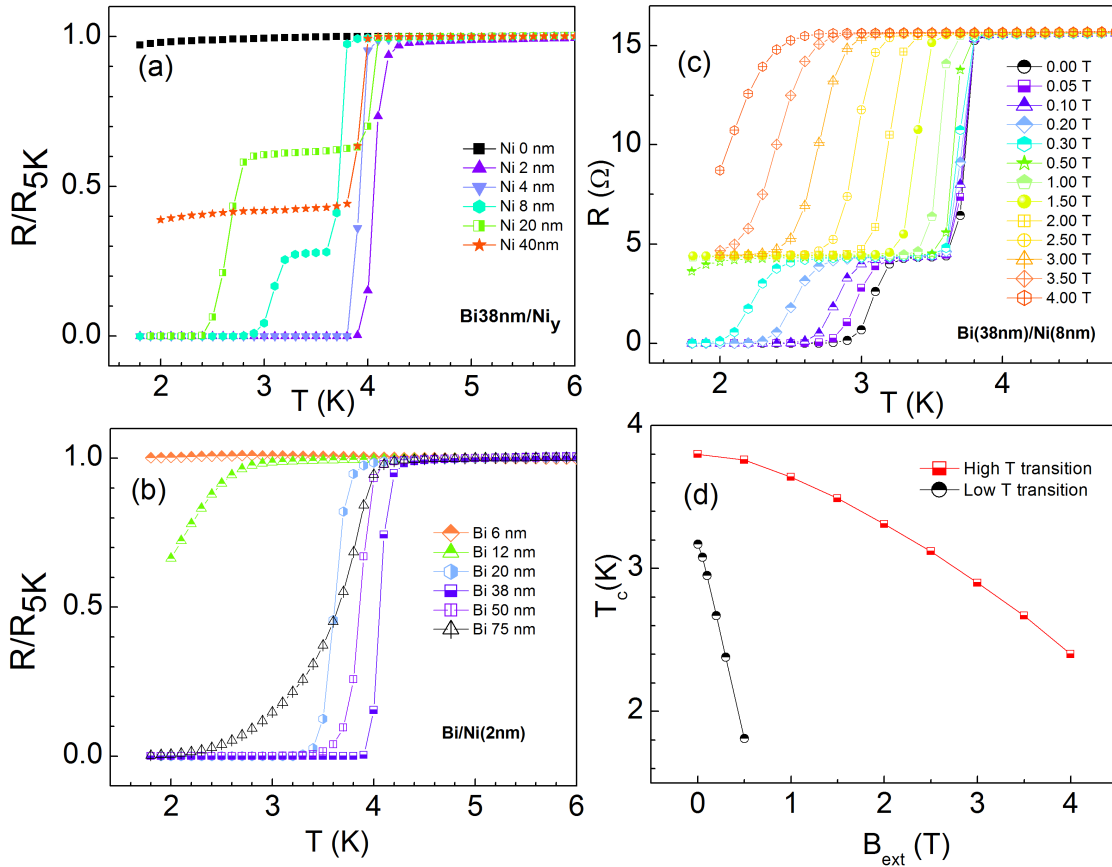


FIG. 1: Normalized resistivity as a function of temperature for samples with (a) fixed thickness of Bi layer and different thicknesses of Ni layers and (b) fixed thickness of Ni layer and different thicknesses of Bi layers. (c) Resistance as a function of  $B_{ext}$  for sample with a two-step transition in  $B_{ext}$ . (d)  $T_c$  as a function of  $B_{ext}$  for the two transitions. The  $T_c$  value is defined as the temperature where  $R = 90\%$   $R_{normal}$ .

In order to better understand this observation, the resistivity in different external mag-

netic fields ( $B_{ext}$ ) has been measured as a function of temperature [see Fig. 1 (c)]. From this figure one can see that  $T_c$  decreases with increase of  $B_{ext}$  as expected. However, the higher temperature transition decreases much slower with increase of  $B_{ext}$  than the lower transition. For  $B_{ext} = 0.5$  T, the lower  $T_c$  transition already has been suppressed to 2 K. From Fig. 1 (d) we can calculate the values of  $dB/dT_c$  for the two transitions to be 2.1 T/K and 0.36 T/K, respectively. The upper critical field at zero temperature [ $B_{c2}(0)$ ] is roughly estimated as 1.1 T for the lower temperature transition and 7.4 T for the higher temperature transition. The former value is very close to that obtained by Siva et al. [ $B_{c2}(0) = 1.4$  T] for the  $NiBi_3$  phase in a similar system[5]. Comparing to the flux-grown  $NiBi_3$  single crystals[19], the  $B_{c2}$  value at 1.8 K is slightly higher (0.5 T to 0.35 T). Therefore, the lower temperature transition could be attributed to the formation of  $NiBi_3$ . The latter value, however, is much higher than  $B_{c2}(0)$  of  $NiBi_3$ . To date, very few studies show  $B_{c2}(0)$  of  $NiBi$  and we cannot compare the data obtained in this work with that of  $NiBi$ , which might be the second superconducting phase in our sample related to the higher temperature transition. The results strongly suggest the existence of two superconducting phases, having a different sensibility to  $B_{ext}$  and therefore, a different sensibility for the Ni layer thickness. In order to confirm these two superconducting phases in the Bi/Ni system, the microstructure of the samples has been studied. In the following we will show the results of these studies.

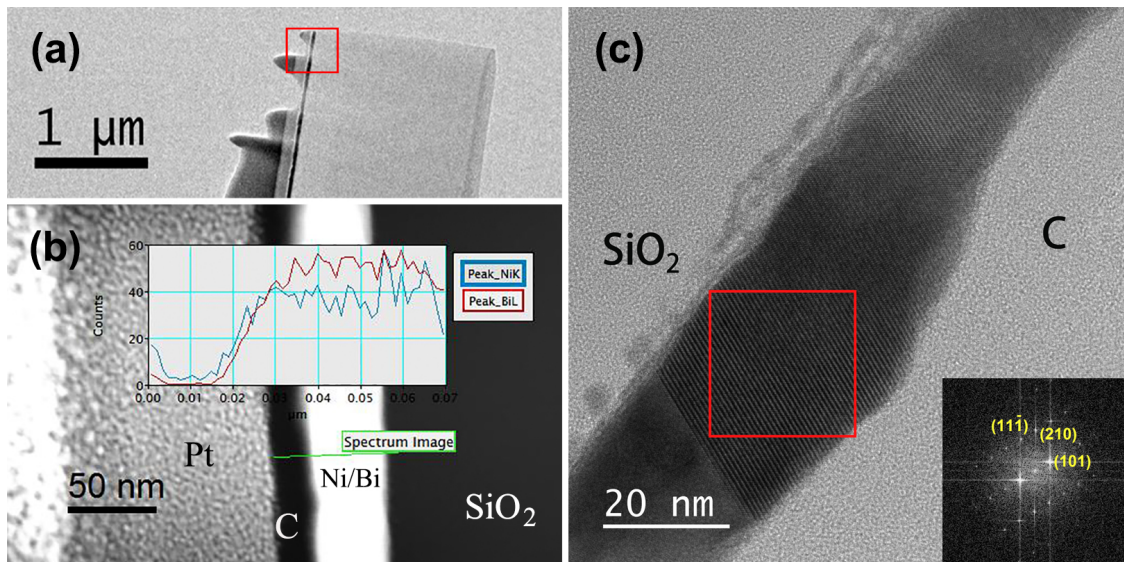


FIG. 2: (a) Low magnification cross-section image of the sample  $Bi_{38}Ni_2$ . (b) HAADF low magnification image and an EDXS linescan of Bi and Ni at the position shown by the line. (c) HRTEM image of the sample. Inset shows the FFT of the image in the square. The structure can be indexed as  $NiBi_3$ .

Fig. 2 shows the cross-section microstructure of the Bi38Ni2 sample. From Fig. 2 (a) one can see that Bi/Ni forms a continuous layer. High Angle Annular Dark Field (HAADF) image [Fig. 2 (b)] shows that there is no contrast difference of the deposited Ni and Bi layer, which indicates that Ni and Bi are mixed. The EDXS linescan clearly shows that when the electron beam scans the Bi/Ni layer, both Ni and Bi are simultaneously detected, having very similar profiles. This confirms that Ni and Bi are homogeneously mixed. The high resolution image [see Fig. 2 (c)] shows that only one layer is observed, i.e., the sample does not have the expected two-layer structure since we first deposited a Bi and then a Ni layer. The Fast Fourier Transform (FFT) of the high-resolution image can be indexed as intermetallic compound NiBi<sub>3</sub>. From these results, we can conclude that Ni and Bi are mixed and form a NiBi<sub>3</sub> phase during deposition by PLD.

Next, the samples with thicker Ni layers (Bi38Ni8, Bi38Ni20 and Bi38Ni40) have also been studied with HRTEM. We know from Fig. 1 that the first two samples show a two-step superconducting transition and the last one a non-complete superconducting transition. The microstructures of the three samples show the same structure: three layers are visible although only a Bi and a Ni layer have been deposited. The TEM results of the Bi38Ni8 and Bi38Ni20 can be found in the supplementary materials. In Fig. 3 we show the results of Bi38Ni40.

With the low magnification image [Fig. 3 (a)] one essentially can only see one layer, however, three layers clearly can be seen in the HR images [Fig. 3 (b)]. The Convergent Beam Electron Diffraction (CBED) results show that the pattern (c) corresponds to the layer marked as 1 in Fig. 3 (b) easily can be indexed as pure fcc Ni. The CBED pattern of the layer in the middle [marked as 2 in Fig. 3(b)] shows that this layer is NiBi<sub>3</sub>, like the structure in Fig. 2. To our surprise, the patterns in (e) cannot be indexed as pure Bi, which we were expecting, since the first layer we deposited was a pure Bi layer. The pattern can be indexed as another intermetallic compound of Ni-Bi: NiBi. This is quite unusual since the Ni rich phase NiBi should be formed near the Ni layer, and not the NiBi<sub>3</sub> layer as we observed. Later we will try to explain why in our case the Bi rich phase NiBi<sub>3</sub> is close to the Ni layer the more Ni rich phase NiBi near the Bi layer (see below).

The sample in addition has been studied by using HRSTEM (model: JEOL ARM) and the results are shown in Fig. 4. From the HR images, one clearly can see the superstructure in the sample. It is interesting to observe that there is a coherent grain boundary between



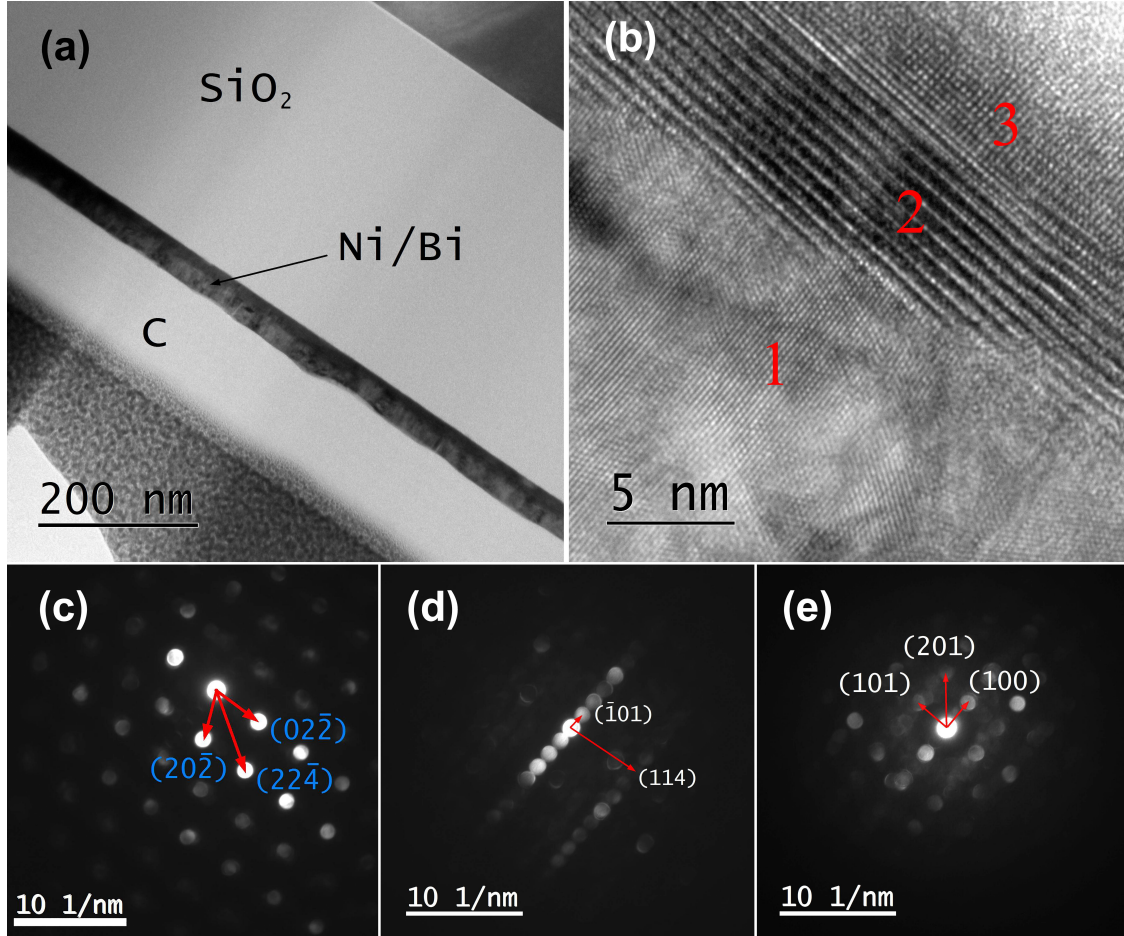


FIG. 3: (a) Low magnification cross-section of the sample Bi<sub>38</sub>Ni<sub>40</sub>. (b) HRTEM image. (c), (d) and (e) are CBED patterns of the structures marked as 1, 2 and 3 in (b).

the superstructure and another phase. Although the planes of the atoms are parallel, the distance between two atomic planes of the superstructure is not double of the distance of the simple structure. The FFT of the image clearly shows that they are from two different crystals with different lattice parameters. The reason for this could be that the concentration of Ni in this crystal is locally different and therefore one part formed NiBi<sub>3</sub> and the other part NiBi. The EDXS line scan results confirm the observation that a Ni rich phase is formed near the substrate. From the elemental profile [Fig. 4 (c)] one can see that the Ni concentration first decreases in the Bi layer and then increases at the interface of Bi/SiO<sub>2</sub>. The Ni elemental mapping [Fig. 4 (d)] shows that the entire interface near SiO<sub>2</sub> has a high Ni concentration. This is in agreement with the CBED results shown in Fig. 3: a Ni rich phase is observed at the interface of SiO<sub>2</sub>. This is not similar to the results of the Bi/Ni interdiffusion studies in literature [23]: there the Ni rich phase NiBi is always near pure Ni

layer and  $\text{NiBi}_3$  is always near pure Bi layer, as indicated in Fig. 4 (e) and (f).

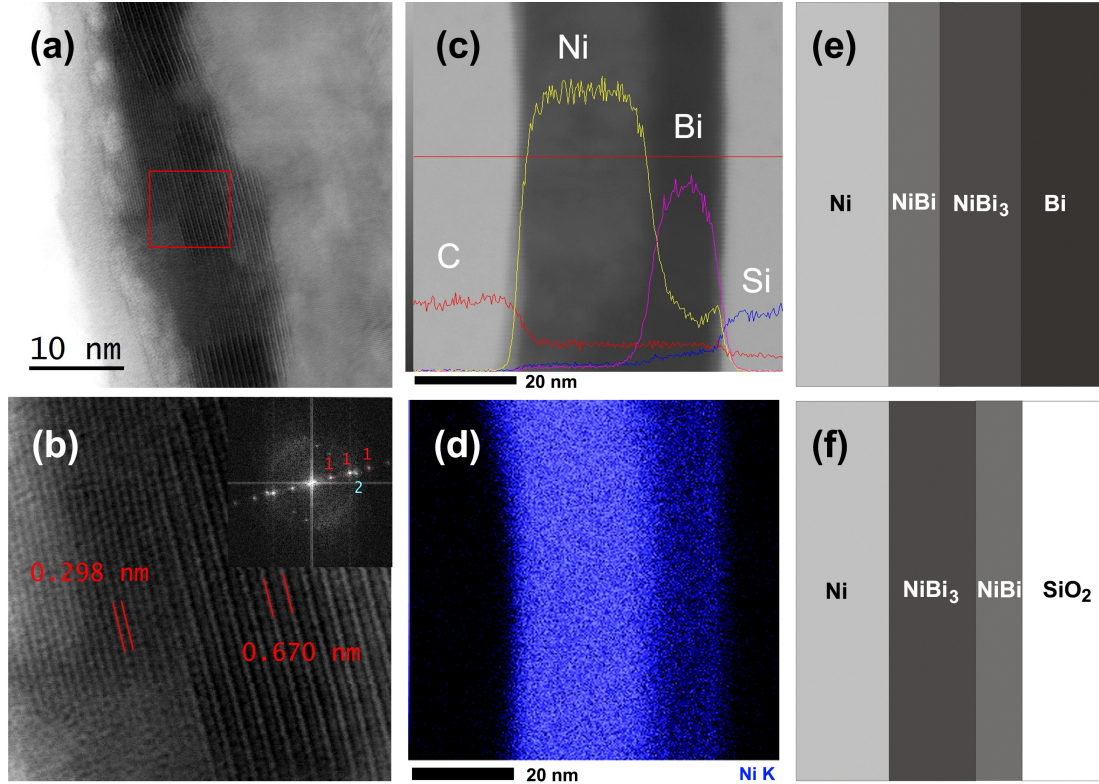


FIG. 4: (a) HR bright field STEM image and (b) Amplification of the red square in (a). The numbers in (b) show the distance between two atomic planes. Inset of (b) shows the FFT of the image and the numbers (1 and 2) indicate that they are from different structures. (c) EDXS linescan of the sample showing the distribution of the elements. An increase of Ni concentration clearly can be seen near the interface of Bi/ $\text{SiO}_2$ . (d) Mapping of Ni, showing the increase of the Ni concentration near the interface of Bi/ $\text{SiO}_2$ . (e) Schematic illustration of the layers resulted from a Bi/Ni interdiffusion, reported in literature. (f) Schematics of the structures formed in this study.

The interpretation is as follows: it is well known that that Bi is a very soft metal and has a very low melting point. The thickness of the Bi layers in this study is only tens of nanometers, which means a very limited number of atomic layers in the direction perpendicular to the surface. In order to accurately perform electric transport measurements, a Si wafer with an insulating  $\text{SiO}_2$  was selected as substrate. Therefore,  $\text{SiO}_2$  lays just below the Bi layer. The growth of thin films by PLD is typically a strong non-equilibrium process [24] and the energy of the atoms arriving at the substrate is quite high. In this case, the Ficks law of diffusion and thermodynamics do not apply to the situation. Although the substrate is at room temperature, when the Ni atoms reach the soft and thin Bi layers, they can easily penetrate it and reach the  $\text{SiO}_2$  layer. As the diffusion coefficient of Ni in  $\text{SiO}_2$  is much smaller than

that in Bi [25, 26], the SiO<sub>2</sub> layer results much harder for Ni atoms to pass through. After penetrating the Bi layer, most of the Ni atoms stop at the interface of Bi/SiO<sub>2</sub> and only very few of them can go into the SiO<sub>2</sub>. As a result, there is a trapping process of Ni atoms at the interface and the deposition process creates a Ni rich region near the substrate of SiO<sub>2</sub>. From the Ni-Bi phase diagram, one knows that the solubility of Ni in Bi is very limited: with the increase of Ni concentration in Bi, first a Bi rich intermetallic compound (NiBi<sub>3</sub>) is formed; with further increase of Ni concentration a Ni rich phase (NiBi) occurs. The unusual Ni concentration gradient obtained as a consequence of the Ni trapping process resulted in the formation of NiBi at the interface of Bi/SiO<sub>2</sub>. This phenomenon needs more detailed studies in the future.

With these results, we confirmed the formation of NiBi<sub>3</sub> during the sample preparation observed by Siva et al. in samples deposited by thermal evaporation[5] and by S.P.Chao et al. in samples prepared by molecular beam epitaxy[11]. Furthermore, we also identified another intermetallic phase (NiBi) in the sample. We can conclude that the formation of NiBi and NiBi<sub>3</sub> is the reason for the observed superconductivity in Bi/Ni system. Ideally, the two superconducting phases should be parallel to the current flow in the electric transport measurements. However, due to the high surface roughness of the first deposited Bi layer (see the low magnification images of Fig. 2 and 3) and diffusion controlled superconducting phase (NiBi<sub>3</sub> and NiBi) formation, the real configuration of the two phases in some of the samples could be NiBi particles or islands embedded in NiBi<sub>3</sub> film. Since T<sub>c</sub> of NiBi<sub>3</sub> is lower than that of NiBi and NiBi<sub>3</sub> is in contact with the Ni layer, T<sub>c</sub> of NiBi<sub>3</sub> decreases more than that of NiBi and as a result, a two-step superconducting transition may appear as shown in Fig. 1. Although we identified two superconducting phases in the above Bi/Ni bi-layers, other interpretations cannot be ruled out with the samples prepared at room temperature only. For that reason we studied two samples prepared at 4.2 K. At that temperature interdiffusion between Ni and Bi is not likely to occur.

## **B. Samples prepared at 4.2 K**

From Fig. 5 (a) one can see that the first Bi layer deposited at 4.2 K is a superconductor with T<sub>c</sub> ~ 6.0 K since it is in an amorphous state [27, 28]. When the temperature increases the amorphous Bi film crystallizes at ~ 20 K (the crystallization temperature depends on

the thickness of the Bi film [29]) to the rhombohedral structure. After annealing the sample at 300K, the Bi film completely lost superconductivity. Now we are sure that there is a crystalline non-superconducting Bi layer on the substrate. The sample then was cooled down to 4.2 K and a 5 nm Ni layer was deposited on top. As shown in Fig. 5 (b), the sample prepared at 4.2 K does not have a superconducting transition down to 1.8 K. Even after annealing at 300 K no superconducting transition has been observed. The resistivity decreases after annealing due to the decrease of the density of defects. This result is completely different from that of samples prepared at room temperature always showing superconductivity.

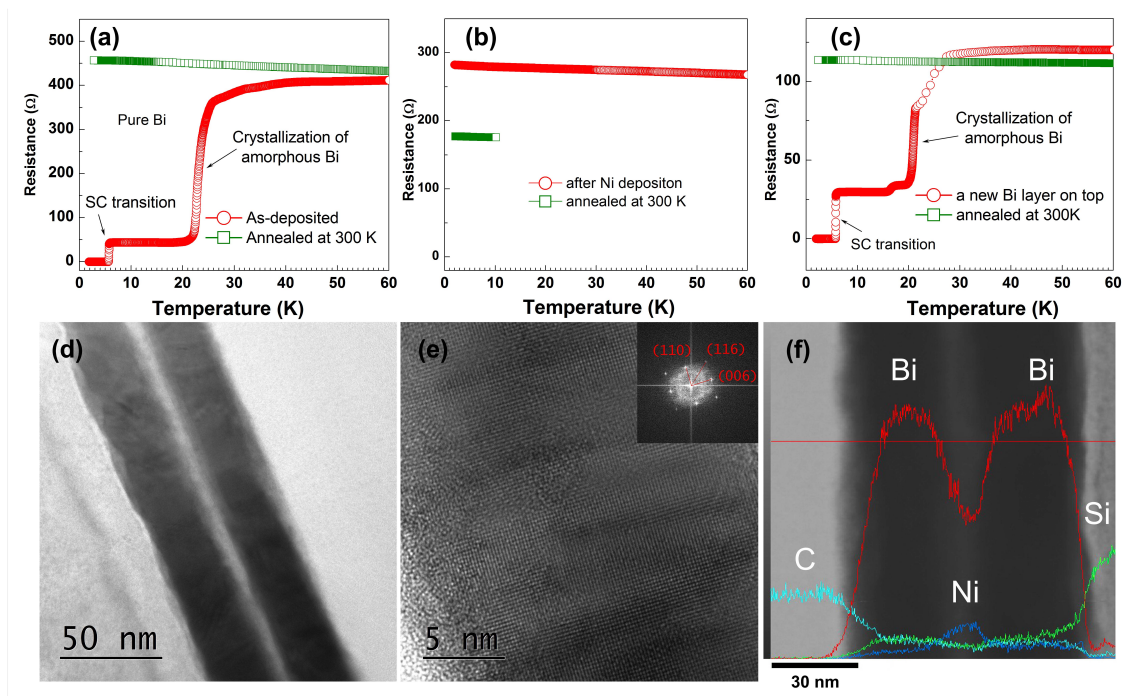


FIG. 5: Resistance as a function of temperature for (a) 35 nm pure Bi layer before and after annealing, showing that the amorphous Bi is superconducting and when it crystallizes to rhombohedral structure it loses superconductivity. (b) Crystalline Bi layer with 5 nm Ni deposited on top at 4.2 K, showing that there is no superconductivity for both as-prepared sample and after annealing at 300 K. (c) A second Bi layer deposited on top of Ni at 4.2 K and then annealed at 300 K in order to have a new interface of crystalline Bi and Ni. (d) Microstructure of the cross-section of Bi/Ni/Bi tri-layers prepared at 4.2 K. (e) High-resolution image of one Bi layer. Inset shows the FFT of the image, which can be easily indexed to rhombohedral Bi structure. (f) STEM image of Bi/Ni/Bi tri-layer sample and EDXS linescan profile of Bi, Ni, C and Si elements. The red straight line indicates the position of EDXS linescan.

In order to give more solid evidence, another layer of Bi had been deposited at 4.2 K and the amorphous Bi shows the expected superconductivity, as shown in Fig. 5 (c). However,

it again loses superconductivity after annealing to 300 K. This shows that the interface of Ni and Bi does not induce superconductivity neither in Bi layer nor in Ni layer.

The cross-section of the low-temperature-prepared sample clearly shows the tri-layer structure, with two Bi layers and one Ni layer in between [as shown in Fig. 5 (d)]. This is confirmed by the EDXS line scan profile in Fig. 5 (f). The HRTEM study shows that the two black layers are rhombohedral Bi layers. No evidence of the formation of NiBi or NiBi<sub>3</sub> was found.

We observed that the Ni layer deposited at 4.2 K is still amorphous after annealing at room temperature. In this sample, there is no crystalline Ni/crystalline Bi interface. Therefore, we cannot rule out the interpretation that the FCC structure of Ni induces FCC Bi, which is a superconductor. For that reason, we did an additional experiment with the results shown in Fig. 6.

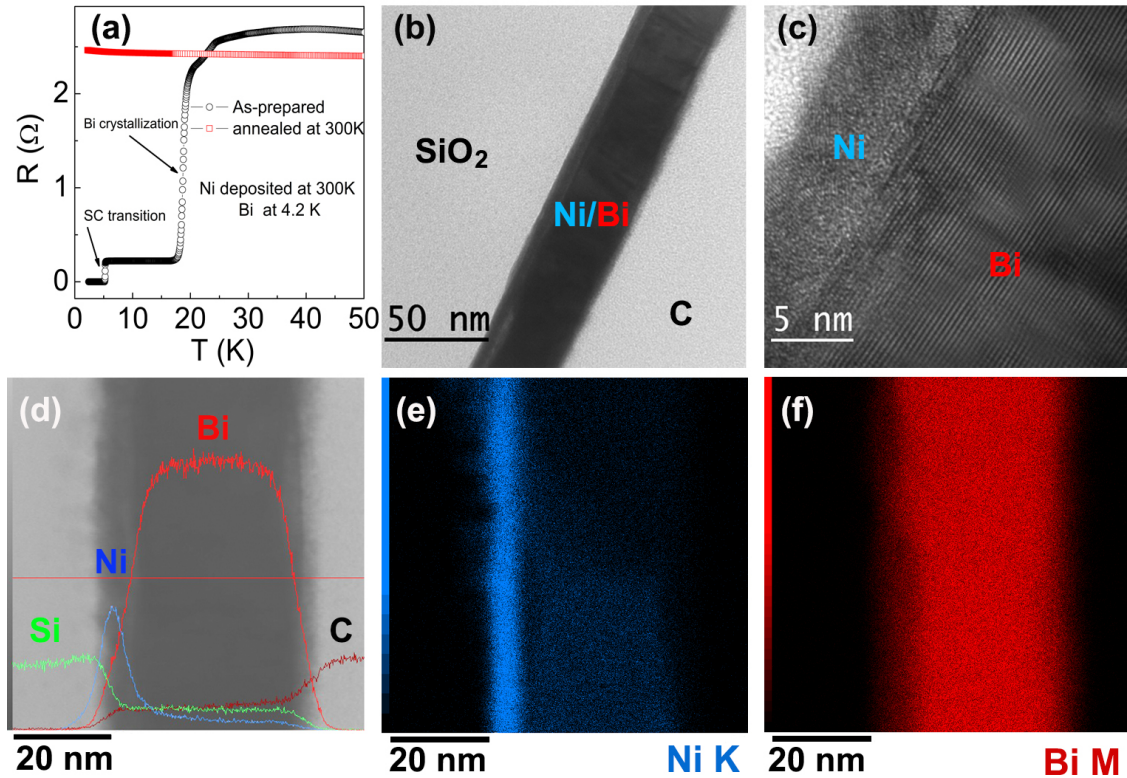


FIG. 6: (a) Resistance as a function of temperature for a sample with Ni deposited at room temperature and Bi deposited at 4.2 K and then annealed at 300 K in order to have a crystalline Ni/Bi interface. (b) Microstructure of the cross-section of Ni/Bi bi-layer with Ni deposited at 300 K and Bi deposited 4.2 K. (c) High resolution image. (d) STEM image and EDXS linescan profile of Bi, Ni, C and Si. The red straight line indicates the position of EDXS linescan. (e) and (f) are the elemental mappings of Ni and Bi, respectively.

The sample has been prepared as following: First a 5 nm thick Ni layer was deposited at room temperature to obtain a FCC Ni thin film. In the following sequence, the sample was cooled down to 4.2 K and, at that temperature, a 40 nm Bi layer was deposited. The resistance for the as-prepared sample was measured when heating the sample up to 300 K [see Fig. 6 (a)]. The first transition at  $\sim 6.0$  K is the superconducting transition of amorphous Bi and the second transition at  $\sim 18$  K is the crystallization of amorphous Bi. After annealing at 300 K, the sample still does not show a superconducting transition down to 2 K.

The microstructure of this sample clearly shows a two-layer structure as shown in Fig. 6 (b). Most importantly, unlike the Ni layer prepared at 4.2 K, the Ni layer prepared at 300 K is crystalline as we expected [see Fig. 6 (c)]. The interface of Ni and Bi clearly can be seen and there is no evidence of FCC Bi near the interface. No NiBi or NiBi<sub>3</sub> as in the samples prepared at room temperature has been observed as well, which indicates that there is no interdiffusion or reaction between Ni and Bi during deposition. From the EDXS line scan and elemental mapping results one can see that the thinner layer is Ni and the thicker layer is Bi.

With all the results of this additional sample, we can conclude that a crystalline Bi/Ni interface has been created and no superconductivity has been observed down to 2 K. We could not identify an FCC Bi phase at the crystalline Bi/Ni interface. Thus, the formation of the FCC Bi phase reported by Moodera et al. [3] is actually rather unlikely to occur as commented by Huslt et al. [30]. As a result, the occurrence of superconductivity at the non-epitaxial crystalline Bi/Ni interface can be ruled out.

#### IV. SUMMARY

For some Bi/Ni bi-layer samples prepared at room temperature by PLD, a two-step superconducting transition has been observed. The HRTEM images and CBED patterns of the cross-section sample reveal that the Ni atoms deposited onto the Bi film react with the Bi and form NiBi<sub>3</sub> and NiBi phases. As one knows that both NiBi<sub>3</sub> and NiBi are superconductors with  $T_c \sim 4.0$  K, these intermetallic compounds are responsible for the superconductivity observed in the Bi/Ni bi-layers prepared by PLD. The observed two-step transition in an external magnetic field shows a different behavior of the two superconducting

phases: NiBi and NiBi<sub>3</sub>.  $T_c$  of one phase decreases much faster than that of the other phase. Unlike the Bi/Ni system studied in literature, the CBED patterns show that in our case NiBi is formed near the Bi layer and NiBi<sub>3</sub> near Ni layer. EDXS analysis confirms that the Ni concentration near the interface of Bi and substrate is higher than in the Bi layer near Ni. This is mainly due to the non-equilibrium and highly energetic process during deposition with PLD.

The samples prepared at 4.2 K show that Bi/Ni bi-layers or Bi/Ni/Bi tri-layers with crystalline Bi layers do not have a superconducting transition down to 1.8 K. Superconductivity only can be observed when the Bi layer is amorphous with  $T_c \sim 6.0$  K. Therefore, the interface of Bi/Ni cannot induce superconductivity in both Bi and Ni layer. The cross-section studies show that the Ni layer deposited at 4.2 K is still amorphous after annealing at room temperature. This experimental observation can rule out the interpretation of the superconductivity in Bi/Ni system attributed to the amorphous Bi layer at the interface of Bi/Ni. The annealed sample with Ni deposited at 300 K and Bi deposited at 4.2 K also does not have a superconducting transition down to 2 K. The quality of the Bi/Ni interface depends on the preparation method. However, all the Bi/Ni bi-layers reported in literature prepared above 110 K are superconducting and the preparation method does not appear to play a role. Furthermore, the superconducting properties show similar characteristics despite of the different interface conditions: the  $T_c$  and its behavior in an external magnetic field are very similar in all of the reported results. Our samples prepared at 4.2 K show that Bi/Ni bi-layers are non-superconducting and the key feature of this experiment is the very low substrate temperature. In this case, one can conclude that the non-epitaxial crystalline Ni/Bi interface without interdiffusion cannot induce superconductivity in Bi/Ni system. Other interpretations of superconductivity in Bi/Ni bi-layers therefore should be double-checked especially when there exist two superconducting intermetallic compounds (NiBi and NiBi<sub>3</sub>) and the Bi properties favour the formation of them. Concerning the long going discussion about the mysterious appearance of superconductivity in Bi/Ni bi-layer systems, our results offer an interpretation that can explain many of the by now open questions.

## ACKNOWLEDGEMENTS

This work was supported by CAPES, CNPq and FAPERJ. The authors thank LaMAR/CAIPE at Universidade Federal Fluminense, LABNANO at Centro Brasileiro de Pesquisas Físicas for the use of their facilities and ANP/PETROBRAS for partial support. The authors thank Prof. J. Litterst for critical reading of this manuscript. This work was performed in part at the Center for Nanoscale Systems (CNS), a member of the National Nanotechnology Coordinated Infrastructure Network (NNCI), which is supported by the National Science Foundation under NSF award no. 1541959.

## SUPPLEMENTARY INFORMATION

The following files are available free of charge.

- CrossSection: Cross-section microstructures of Bi<sub>38</sub>Ni<sub>8</sub> and Bi<sub>38</sub>Ni<sub>20</sub>.

- 
- [1] N. Kurti and F. Simon, Proceedings of the Royal Society of London A: Mathematical, Physical and Engineering Sciences **151**, 610 (1935), <http://rspa.royalsocietypublishing.org/content/151/874/610.full.pdf>.
- [2] L. Esaki and P. J. Stiles, Phys. Rev. Lett. **14**, 902 (1965).
- [3] J. Moodera and R. Meservey, Physical Review B **42**, 179 (1990).
- [4] P. LeClair, J. S. Moodera, J. Philip, and D. Heiman, Phys. Rev. Lett. **94**, 037006 (2005).
- [5] V. Siva, K. Senapati, B. Satpati, S. Prusty, D. K. Avasthi, D. Kanjilal, and P. K. Sahoo, Journal of Applied Physics **117**, 083902 (2015), <http://dx.doi.org/10.1063/1.4913267>.
- [6] X. X. Gong, H. X. Zhou, P. C. Xu, D. Yue, K. Zhu, X. F. Jin, H. Tian, G. J. Zhao, and T. Y. Chen, Chinese Physics Letters **32**, 067402 (2015).
- [7] V. I. Petrosyan, V. N. Molin, O. I. Vasin, P. A. Skripkina, S. I. Stenin, and E. G. Batyev, Soviet Journal of Experimental and Theoretical Physics **39**, 485 (1974).
- [8] X. Gong, M. Kargarian, A. Stern, D. Yue, H. Zhou, X. Jin, V. M. Galitski, V. M. Yakovenko, and J. Xia, Science Advances **3** (2017), 10.1126/sciadv.1602579, <http://advances.sciencemag.org/content/3/3/e1602579.full.pdf>.



- [9] H. Zhou, X. Gong, and X. Jin, *Journal of Magnetism and Magnetic Materials* **422**, 73 (2017).
- [10] S. H. Gonsalves, J. A. F. H. L. Monteiro, A. C. D. S. Leal, A. A. V. C. d. Andrade, G. B. d. Souza, E. C. Siqueira, F. C. Serbena, and A. R. Jurelo, *Materials Research* (2017), 10.1590/1980-5373-mr-2016-0538.
- [11] S. Chao, S. C. LU, J. H. LIN, P. CHIU, W. J. LI, P. J. CHEN, Y. LIOU, and T. K. LEE, *APS March Meeting 2017* **62**, R45.00006 (2017).
- [12] B. T. Matthias, *Phys. Rev.* **92**, 874 (1953).
- [13] P. Nedellec, F. Creppy, L. Dumoulin, and J. Burger, *Physics Letters A* **111**, 67 (1985).
- [14] P. S. Neelakanta, *Handbook of electromagnetic materials: monolithic and composite versions and their applications*, Neelakanta95 (CRC press, 1995).
- [15] Y. Fujimori, S. ichi Kan, B. Shinozaki, and T. Kawaguti, *Journal of the Physical Society of Japan* **69**, 3017 (2000), <http://dx.doi.org/10.1143/JPSJ.69.3017>.
- [16] S. Park, K. Kang, W. Han, and T. Vogt, *Journal of Alloys and Compounds* **400**, 88 (2005).
- [17] J. Kumar, A. Kumar, A. Vajpayee, B. Gahtori, D. Sharma, P. K. Ahluwalia, S. Auluck, and V. P. S. Awana, *Superconductor Science and Technology* **24**, 085002 (2011).
- [18] X. Zhu, H. Lei, C. Petrovic, and Y. Zhang, *Phys. Rev. B* **86**, 024527 (2012).
- [19] B. Silva, R. F. Luccas, N. M. Nemes, J. Hanko, M. R. Osorio, P. Kulkarni, F. Mompean, M. García-Hernández, M. A. Ramos, S. Vieira, and H. Suderow, *Phys. Rev. B* **88**, 184508 (2013).
- [20] D. P. Norton, “Pulsed laser deposition of complex materials: Progress toward applications,” in *Pulsed Laser Deposition of Thin Films* (John Wiley & Sons, Inc., 2006) pp. 1–31.
- [21] S. Rubin, M. Holdenried, and H. Micklitz, *Eur. Phys. J. B* **5**, 23 (1998).
- [22] Y. T. Xing, H. Micklitz, T. G. Rappoport, M. V. Milošević, I. G. Solórzano-Naranjo, and E. Baggio-Saitovitch, *Phys. Rev. B* **78**, 224524 (2008).
- [23] M. S. Lee, C. Chen, and C. R. Kao, *Chemistry of Materials* **11**, 292 (1999).
- [24] D. Bäuerle, *Laser Processing and Chemistry*, Bauerle11 (Springer Berlin Heidelberg, 2011).
- [25] R. N. Ghoshtagore, *Journal of Applied Physics* **40**, 4374 (1969).
- [26] V. Dybkov and O. Duchenko, *Journal of Alloys and Compounds* **234**, 295 (1996).
- [27] D. B. Haviland, Y. Liu, and A. M. Goldman, *Phys. Rev. Lett.* **62**, 2180 (1989).
- [28] W. T. Herrera, I. S. Dinola, M. A. Continentino, H. Micklitz, Y. T. Xing, M. B. Fontes, and E. Baggio-Saitovitch, *The European Physical Journal B* **86**, 508 (2013).

- [29] G. Bai, R. Li, H. Xu, Y. Xia, Z. Liu, H. Lu, and J. Yin, *Physica B: Condensed Matter* **406**, 4436 (2011).
- [30] J. A. van Hulst, G. Rietveld, D. van der Marel, F. Tuinstra, and H. M. Jaeger, *Phys. Rev. B* **47**, 548 (1993).